Reviewed research article

The explosive, basaltic Katla eruption in 1918, south Iceland II. Isopach map, ice cap deposition of tephra and layer volume

Magnús Tumi Gudmundsson[1,2], Maria H. Janebo[1], Guðrún Larsen[1], Thórdís Högnadóttir[1], Thorvaldur Thordarson[1,2], Jónas Gudnason[3] and Tinna Jónsdóttir[4]

[1]*Nordvulk, Institute of Earth Sciences, University of Iceland, Sturlugata 7, IS-102 Reykjavík, Iceland*

[2]*Faculty of Earth Sciences, University of Iceland, Sturlugata 7, IS-102 Reykjavík, Iceland*

[3]*Landsvirkjun, Háaleitisbraut 68, 108 Reykjavík, Iceland*

[4]*Orkustofnun, Grensásvegi 9, 108 Reykjavík, Iceland*

Corresponding author mtg@hi.is; https://doi.org/10.33799/jokull2021.71.021

Abstract — *Due to poor preservation and lack of proximal tephra thickness data, no comprehensive isopach map has existed for the tephra layer from the major eruption of the Katla volcano in 1918. We present such a map obtained by combining existing data on the thickness of the 1918 tephra in soil profiles with newly acquired data from the 590 km^2 Mýrdalsjökull ice cap which covers the Katla caldera and its outer slopes. A tephra thickness of 20–30 m on the ice surface proximal to the vents is inferred from photos taken in 1919. The greatest thicknesses presently observed, 30–35 cm, occur where the layer outcrops in the lowermost parts of the ablation areas of the Kötlujökull and Sólheimajökull outlet glaciers. A fallout location within the Katla caldera is inferred for the presently exposed tephra in both outlet glaciers, as estimates of balance velocities imply lateral transport since 1918 of ∼15 km for Kötlujökull, ∼11 km for Sólheimajökull and about 2 km for Sléttjökull. Calculations of thinning of the tephra layer during this lateral transport indicate that the presently exposed tephra layers in Kötlujökull and Sólheimajökull were respectively over 2 m and about 1.2 m thick where they fell while insignificant thinning is inferred for the broad northern lobe of Sléttjökull. The K1918 layer has an estimated volume of 0.95±0.25 km^3 (corresponding to 1.15±0.30×10^{12} kg) whereof about 50% fell on Mýrdalsjökull. About 90% of the tephra fell on land and 10% in the sea to the south and southeast of the volcano. The volume estimate obtained contains only a part of the total volume erupted as it excludes water-transported pyroclasts and any material that may have been left on the glacier bed at the vents. While three main dispersal axes can be defined (N, NE and SE), the distribution map is complex in shape reflecting tephra dispersal over a period of variable wind directions and eruption intensity. In terms of airborne tephra, Katla 1918 is the largest explosive eruption in Iceland since the silicic eruption of Askja in 1875.*

INTRODUCTION

The eruption of Katla in 1918 (October 12–November 4) with its extensive tephra fallout and a massive jökulhlaup, caused by intense ice melting of the overlying glacier during the first phase of the eruption, belongs to one of the most prominent natural events that occurred in Iceland in the 20th century. Due to Katla's proximity to inhabited areas, with its 100 km^2 ice-filled caldera beneath the Mýrdalsjökull ice cap, past eruptions with the associated jökulhlaups have had major impact on the neighboring farming districts (e.g. Thorarinsson, 1975; Larsen, 2000; 2018). For the same reasons, Katla remains one of the most dangerous volcanoes in Iceland (Gudmundsson *et al.*, 2008) calling for large monitoring networks and detailed response plans (e.g. Þorkelsson *et al.*, 2005).

Extensive work has been carried out over the past decades to study Katla and its eruptions, notably the eruption history through tephrochronology and other tephra studies (e.g. Thorarinsson, 1975; Larsen, 2000; Larsen *et al.*, 2001; Óladóttir *et al.*, 2008; 2014; 2018; Schmith *et al.*, 2018), studies of the jökulhlaup of 1918 (Tómasson, 1996; Duller *et al.*, 2008; Larsen, 2018), glacier and ice bedrock mapping on Mýrdalsjökull (Björnsson *et al.*, 2000; Mackintosh *et al.*, 2000) and through various geophysical monitoring and research (e.g. Einarsson and Brandsdóttir, 2000; Jónsson and Kristjánsson, 2000; Gudmundsson *et al.*, 1994; Sturkell *et al.*, 2007). However, until now, no comprehensive isopach map has existed for the tephra layer formed in 1918.

Conditions for tephra preservation for the Katla 1918 tephra layer were not favourable over large parts of the fallout area, which includes large regions of vegetation-poor highlands and sandur plains in the lowlands. The eruption occurred in late autumn, after the growth period of vegetation. Snow cover is patchy and sporadic in south Iceland in the autumn months, a period of frequent strong winds. These effects contribute to low preservation potential of the tephra. Fallout occurred over an extended period. The most intense fallout in inhabited areas occurred during 12–14 and 22–24 October (Larsen *et al.*, this issue). All of the above resulted in a complicated distribution pattern and considerable variation in tephra thickness in soils. In addition, limited information has been available on tephra thicknesses on the ice cap. The 1918 tephra has been preserved in Mýrdalsjökull and can be accessed on most of the outlet glaciers of the 590 km^2 ice cap. In 2018, on the 100^{th} anniversary of the eruption, an effort was made to sample the tephra in Mýrdalsjökull and its immediate surroundings as well as analyse the existing contemporary information on conditions at and around the vents in the south-eastern part of the Katla caldera. In this paper, we combine the results of this work with the extensive data on the Katla 1918 tephra layer to compile an isopach map and estimate the volume of tephra erupted. An overview of contemporary records of tephra fallout and of the jökulhlaup is provided in the complementary paper by Larsen *et al.* (this issue).

THE KATLA 1918 ERUPTION

The eruption of Katla in 1918 began on October 12. It was preceded by earthquakes that were felt in Mýrdalur. Around 3 PM, an eruption plume was seen rising from Mýrdalsjökull and shortly after a catastrophic jökulhlaup was observed propagating down the outwash plain of Mýrdalssandur to the east of the volcano, carrying huge amounts of water-transported pyroclasts and sediment (e.g. Jóhannsson, 1919; Tómasson, 1996). Contemporary measurements from Reykjavík indicate a 14 km high plume in the late afternoon (Eggertsson, 1919). The initial phase was subglacial with extremely high melting rates. The visible eruption was preceded by sound of running water by 1.5–2 hours and seismic tremor by $\sim$3.5 hours (Larsen *et al.*, this issue). This indicates that the subglacial phase lasted 2–3.5 hours. The main jökulhlaup was over by the morning of October 13, while the eruption continued until the first days of November, ending on November 4. Fallout persisted throughout with varying intensity (Larsen *et al.*, this issue) and tephra was dispersed in all directions, with the heaviest fallout occurring to the north and northeast of the volcano. Tephra fallout was detected in most parts of Iceland (Larsen *et al.*, this issue). In terms of tephra volume and jökulhlaup size, Katla 1918 has been classified as belonging to the larger eruptions of Katla in the last thousand years (Larsen, 2000; Gudmundsson *et al.*, 2005). The vents that melted through the glacier were located in the southeastern part of the Katla caldera, near the eastern rim, along a 1–2 km long volcanic fissure (Larsen and Högnadóttir, this issue; Larsen *et al.*, this issue).

The magma erupted in 1918 was basaltic, typical for eruptions from Katla (e.g. Óladóttir *et al.*, 2008). The tephra is relatively fine-grained, showing clear evidence of brittle fragmentation by magma-water interaction for long periods during the eruption (Jónsdóttir, 2015).

DATA AND METHODS

Thickness measurements of the Katla 1918 layer have been made over several decades in soil sections. Figure 1 summarises the data used for compilation of the isopach map. Sigurður Þórarinsson published mea-

surements from over 60 locations in the period 1940–1981 (e.g. Bjarnason and Thorarinsson, 1940; Thorarinsson, 1944, 1958, 1968, 1981) and the present authors have made additional measurements at 290 locations (Figure 1). The scarcity of data in the area beyond 60 km distance north of Katla is due to the very poor preservation in these mostly barren highlands. Contemporary records demonstrate that minor fallout occurred in most parts of the country (Larsen *et al.*, this issue). For the more distal and more recent surveys, samples have been taken and the origin of the tephra confirmed by microprobe analyses.

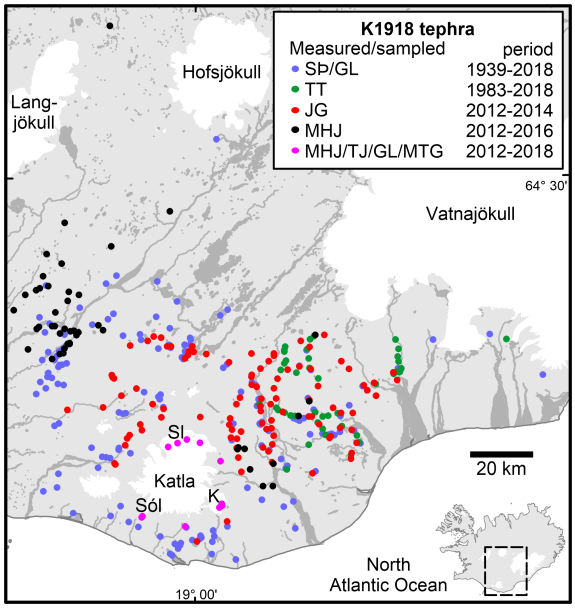

Figure 1. Katla 1918, sampling locations and overview of sampling 1939–2018. Only points where the layer was detected are included on the map. The outlet glaciers of Mýrdalsjökull are indicated: Sól: Sólheimajökull, K: Kötlujökul, Sl: Sléttjökull. – *Sýnatökustaðir þar sem gjóskulagið frá Kötlugosinu 1918 hefur fundist. Elstu mælingarnar eru frá 1939 en þær síðustu frá 2018.*

On Mýrdalsjökull we have sampled the 1918 tephra and measured the thicknesses in the outlet glaciers of Sólheimajökull, Kötlujökull and Sléttjökull (Figure 1). The tephra on these outlet glaciers was deposited on the accumulation area of Mýrdalsjökull, where it was buried and transported within the glacier by flow until it emerges when surface melting exposes the layer. In the ablation area the exposed tephra layer forms a distinct band, aligned perpendicular to ice flow, extending across the outlet glacier. During summer, meltwater on the ice surface may transport parts of the tephra away, especially the fines (Jónsdóttir, 2015). In order to prevent possible loss of fines from the tephra layer, samples were acquired, either by: (1) cutting out the tephra from the ice with a chainsaw, or (2) by sampling the layer right at the point where it becomes exposed by the ice melting. At Sléttjökull the tephra forms a near continuous layer mixed with some ice. In contrast, at Kötlujökull and Sólheimajökull, the tephra in the ice emerges as a 1–2 m thick layer of ice and tephra. The ice is melted by ablation, leaving an exposed 30–35 cm thick layer of compacted tephra on the glacier surface. This 1–2 m thick layer formed as a mix of snow accumulation and fallout of tephra; contemporary observations indicate repeated snowfall on Mýrdalsjökull over the 23 days of the eruption (Sveinsson, 1919; Jóhannsson, 1919).

Additional estimates of the thickness of tephra within the caldera at the end of the eruption are based on the analysis of photos taken in September 1919 (Gudmundsson and Högnadóttir, 2001) and calculations based on estimates of annual mass balance, balance velocities and layer thinning during ice flow using our measurements in Sólheimajökull and Kötlujökull.

Surface velocity measurements and submeter DGPS measurements on Mýrdalsjökull, over a period of 109 days (12 May–29 August) in the summer of 2001, were used for comparison with calculated ice flow velocities.

TEPHRA THICKNESS ON MÝRDALSJÖKULL

Observations in the Katla caldera in 1919

Conditions in the Katla caldera after the eruption were explored in three separate inspection trips to the eruption site in the summer and autumn of 1919 (G. Sveinsson, 1919; P. Sveinsson, 1930; Jónsson, 2008). The photos taken by Kjartan Guðmundsson on 23

June and 12 September 1919 (Figure 2) have been particularly useful.

The photo taken on 12 September 1919, about 10 months after the eruption ended (Figure 2a), shows thick piles of tephra. In contrast, on the photo from the glacier-covered southern rim of the Katla caldera (Háabunga), taken in June 1919 (Figure 2b), and other similar photos from the same trip (Gudmundsson and Högnadóttir, 2001) the surface is covered by the 1918–19 winter accumulation of snow, which in spring is usually close to 10 m thick in the caldera (Ágústsson *et al.*, 2013). Figure 2a shows the region where the easternmost crater was located and the area to the east of the inferred eruption site. The most conspicuous feature is the canyon that cuts across from left to right (from west to east). A thick layer of tephra covers the landscape and ice is exposed only in few places, notably in the steep lower slopes of the canyon. To the north of the canyon the surface is covered by what remained of the snow layer from the winter of 1918–19, expected to have been a few metres thick at the end of summer. New snow, presumably fallen hours or days before the photo was taken, partly drapes the snow from 1918–19 and parts of the tephra-covered landscape. Despite the chaotic landscape of ice and tephra in the foreground, crevasses are not visible. The area in the upper right hand (northeast) corner is the heavily crevassed steep northern part of the Kötlujökull outlet glacier, where it flows out of the caldera, about 3–4 km away. The photos taken by Kjartan Guðmundsson on 23 June 1919 (Figure 2b), when visibility was good, show that this northern part of the outlet glacier was more or less intact and not much altered by the eruption, apart from being covered with tephra.

The west-east canyon seen on Figure 2a extended into the southern part of the outlet glacier where it flows out of the caldera. The explorers in 1919 (Jónsson, 2008) were of the opinion that the bottom of the canyon marked the glacier bed. However, radio-echo soundings have revealed that ice thickness where most of the canyon was located in 1919 reaches several hundred meters (Björnsson *et al.*, 2000; Pálsson *et al.*, 2005). Thus, although having a floor of tephra, the canyon was cut into both the tephra cover and the underlying glacier, with ice underneath the tephra-covered bottom. The most likely explanation for the formation of the canyon is supraglacial drainage of meltwater in the first 1–2 km of the path of meltwater from the vents towards east, down towards the outlet glacier. Such supraglacial flow of meltwater was observed in the Gjálp eruption in 1996 (Gudmundsson *et al.*, 2004) and did also occur in the first days of the Eyjafjallajökull eruption in 2010 (Magnússon *et al.*, 2012; Oddsson *et al.*, 2016). Although the canyon in Katla and its surroundings have similarities with the Gjálp ice canyon, the thickness of tephra on this photo appears an order of magnitude greater than the maximum seen at Gjálp (1–2 m). A series of scaled comparisons permits a tephra thickness estimate as follows: A small stream, probably a few meters wide, can be seen flowing along the bottom of the canyon on the western (left hand) side. According to an estimate made by the explorers in September 1919, who descended to the bottom of the canyon, the stream had a discharge of 0.2–0.3 m^3/s (Jónsson, 2008). The tephra in the walls of the canyon has a thickness that is several times the width of the stream at the bottom. Further rough scaling can be obtained from the observations made in 1919, where the canyon is said to have been 1–2 km long and at most 200 m wide at the top (Jónsson, 2008). The photograph (Figure 2a) is taken approximately 1 km south of the main leg of the canyon, which on the photo trends perpendicular to the line of sight. The dimensions indicated by the photo and the observations from 1919, suggest that the canyon was 50–70 m deep relative to the area immediately to its north. The absence of any visible ice in the upper half of the canyon wall suggests that the tephra pile was not less than one third of the total wall height in the western part of the canyon, and perhaps as much as half the height. This indicates tephra thickness at this site in the range 15–35 m, a few hundred meters away from the vents. Thus, we consider that 25 ± 10 m is a conservative estimate of the maximum tephra thickness outside of the craters.

The 1919 photos and the descriptions of the explorers (Sveinsson, 1919 p. 54–59), together with photos of the plume taken from known locations around the village of Vík (Larsen and Högnadóttir, this issue),

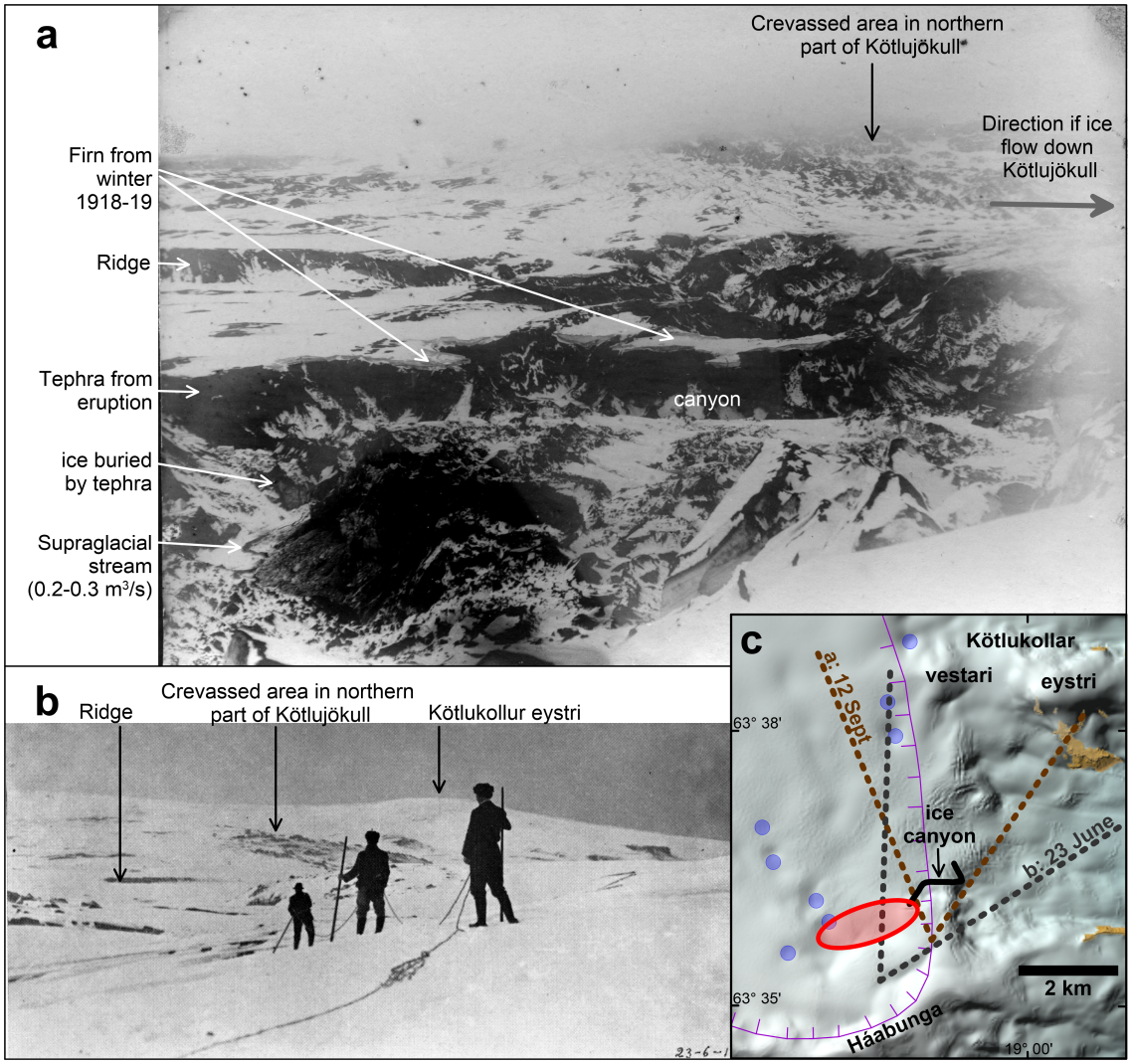

Figure 2. a) The glacier surface near the vents on 12 September 1919, about 10 months after the eruption ended. View northward from the northern slopes of Háabunga, showing a landscape of thick tephra with a canyon cut into it and into the underlying glacier surface. b) View showing the same area as in (a) but from a slightly greater distance, taken on 23 June 1919. Photos in a) and b) taken by Kjartan Guðmundsson. c) Map of present-day topographic features, eruption site of 1918 (red) and approximate location of where photos were taken and areas seen on each photo. The crooked black line marks the location of the ice canyon in 1919. The blue circles are present-day ice cauldrons formed by subglacial geothermal activity. – *a) Yfirborð jökulsins nærri gígunum 1918, myndin er tekin 12. september 1919, 10 mánuðum eftir að gosinu lauk. Þykkir bunkar af gjósku liggja á jöklinum og gilið er að hluta grafið í gjóskuna og að hluta í jökulinn undir. b) Myndin frá 23. júní 1919. Hún sýnir sama svæði og a) en er tekin aðeins fjær og með aðeins austlægari stefnu. c) Brotnar línur afmarka svæðin sem sjást á hvorri ljósmynd, rauðlitaða svæðið sýnir legu gíganna frá 1918 og svarta krókótta línan hvar gljúfrið var 1919. Bláfylltu hringirnir eru sigkatlar.*

constrain the location of the vents in the easternmost part of the caldera, 1.5–2 km to the north of Háabunga (Figure 2). Ice thickness is least at the eastern end, 270–300 m (Björnsson *et al.*, 2000; Pálsson *et al.*, 2005).

Thickness based on the preserved tephra layer

The Katla 1918 tephra is exposed in the lower parts of the ablation areas of all outlet glaciers of Mýrdalsjökull, in most places 1–2 km from the glacier margin (Figures 3 and 4). In order to use the exposed tephra in the outlet glaciers to estimate thickness at the locations where the tephra fell, the relation between the thickness observed in the outlet glaciers today and the thickness at the time of deposition is needed. The distance that the exposed tephra has been transported since 1918 is, furthermore, needed to determine the locations where the tephra fell.

To a first approximation, we assume that the concept of balance velocity (e.g. Cuffey and Paterson, 2010) can be used. The balance velocity at a certain point on a glacier is defined as the depth-averaged horizontal velocity of glacier flow needed to transport the combined net mass balance (amount of snow accumulated minus the amount of surface melting) in the upslope part of the glacier. Our estimate of the balance velocity used here is constrained by mass balance measurements in the Katla caldera (Ágústsson *et al.*, 2013; Eyþórsson, 1945), estimates of the approximate location of the equilibrium lines for each of the three outlet glaciers Kötlujökull (1000 m a.s.l.), Sólheimajökull (1100 m a.s.l.) and Sléttjökull (1000 m a.s.l.) (Björnsson, 1979; Jaenicke *et al.*, 2006), and information on bedrock geometry and ice thickness on Mýrdalsjökull (Björnsson *et al.*, Mackintosh *et al.*, 2000; Pálsson *et al.*, 2005). A slightly negative net mass balance for the Sólheimajökull and Kötlujökull and their accumulation areas of -0.2 to -0.3 m is used, broadly in agreement with the results of Belart *et al.* (2020) on the geodetic mass balance of Mýrdalsjökull over the last 60 years.

Only a rough first order estimate is used for Sléttjökull. It is a broad ice lobe that has retreated significantly over the last 100 years. The lobe-like geometry results in regular ice flow with velocities estimated in the range 15–20 m/year around the equilibrium line, and displacements of ∼2 km over the 100 years between 1918 and 2018 (Figure 4). This is in line with the results of Mayer *et al.* (2016) who measured horizontal velocity of 13 m/year for 2013–14 where the tephra layer outcrops in the upper part of the ablation area near the central part of Sléttjökull.

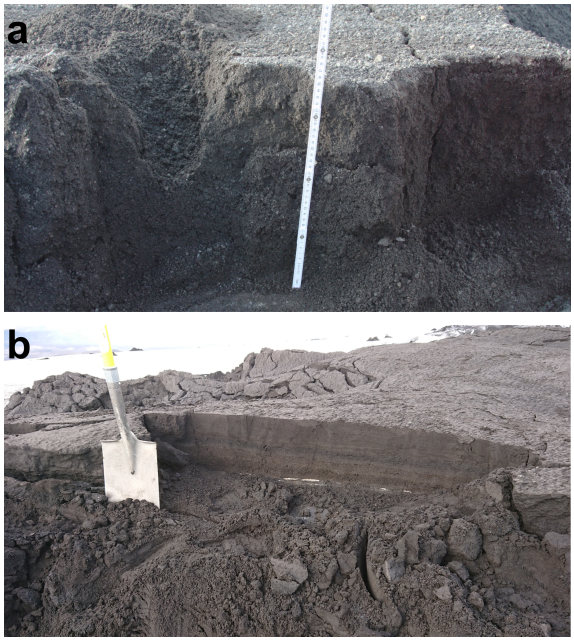

Figure 3. The Katla 1918 tephra layer in Mýrdalsjökull. a) In Kötlujökull on 2 September 2012, the layer is 35 cm thick. b) The 20 cm thick layer on 17 August 2018 at sampling location 2 in Sléttjökull (see Figures 1 and 4a for locations). – *Gjóskulagið frá 1918 á Kötlujökli 2. september 2012, 35 cm þykkt (a) og í Sléttjökli 17. ágúst 2018, 20 cm þykkt (b).*

For both Kötlujökull and Sólheimajökull (Figure 4) the ice that accumulates within the caldera flows through relatively narrow passages (Björnsson et al., 2000; Pálsson *et al.*, 2005) and down the outlet glaciers, resulting in rising flow velocities in the accumulation areas that peak near the equilibrium line. Surface ablation measurements near the terminus of Sólheimajökull since 2013, carried out by students in glaciology at the University of Iceland

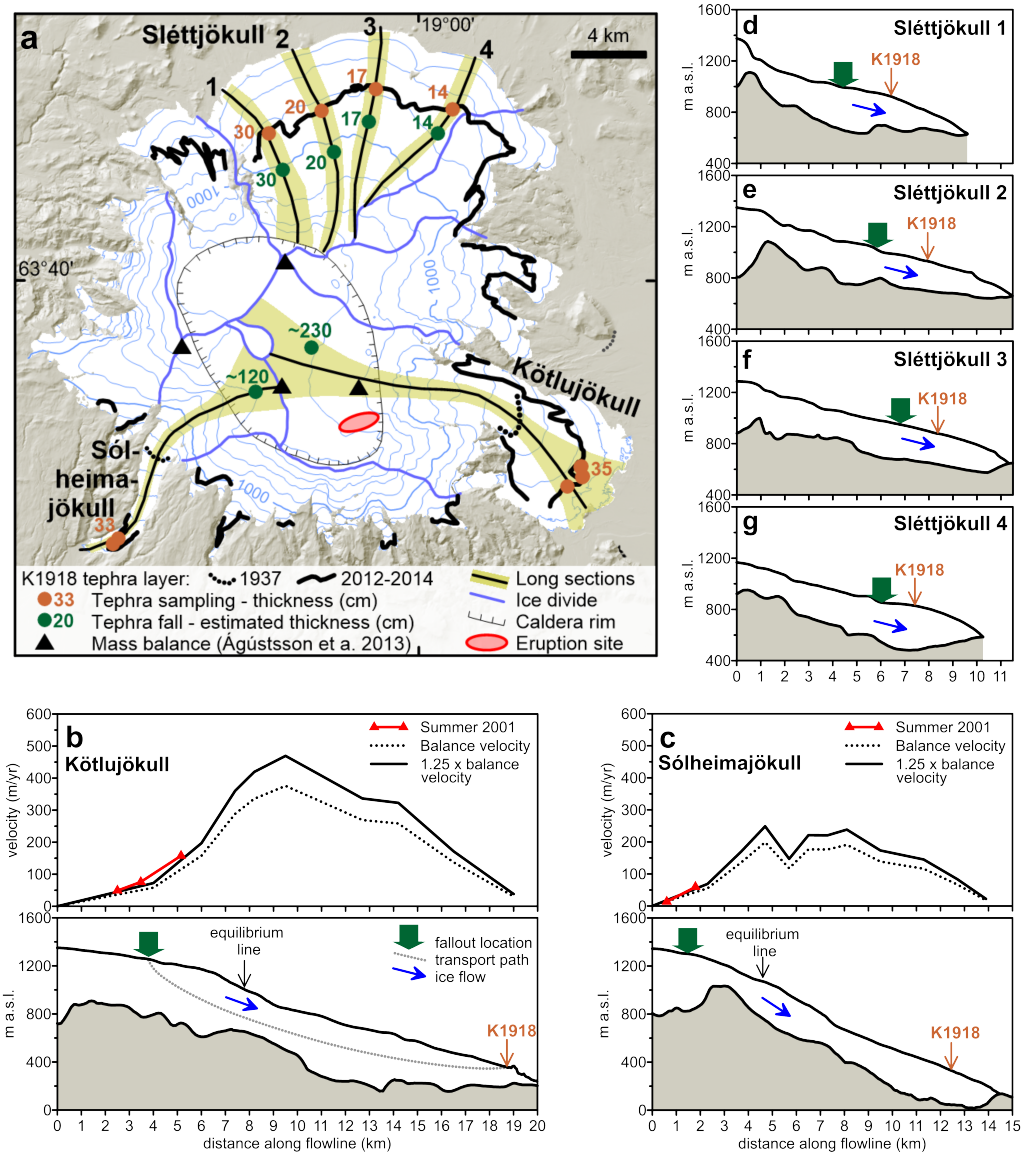

Figure 4. a) Mýrdalsjökull, ice drainage basins (after Björnsson et al., 2000), the 1918 tephra as exposed in the ice, approximate present day ice flow-lines passing through the sampling sites and the estimated location of fallout in 1918. b)-c) Lower panels: cross-sections down Kötlujökull and Sólheimajökull and the approximate path of the K1918 tephra, upper panels: measured surface ice flow in 2001 and estimated balance velocity. d)-g) Cross-sections through sampling sites on Sléttjökull. Bedrock from Björnsson (2000) and Pálsson *et al.* (2005), surface profiles after Lidar map from 2011 (Jóhannesson *et al.*, 2013). – *a) Ísasvæði í Mýrdalsjökli, lega gjóskulagsins frá 1918 í skriðjöklunum, sýnatökustaðir og ísflæðilínur. b) Kötlujökull og c) Sólheimajökull: Neðri mynd: Þversnið eftir flæðilínu og færsla gjóskulagsins frá 1918. Efri mynd: Jafnvægishraði eftir þversniði, bæði meðalhraði og líklegur mesti hraði eftir miðlínu jökulsins ásamt samanburði við yfirborðsmælingar sumarið 2001. d-g) Þversnið eftir ísflæðilínum á Sléttjökli.*

(http://earthice.hi.is/node/900) indicate a net negative balance close to -10 m a^{-1} at 200–300 m a.s.l. No other mass balance measurements have been carried out for the ablation of the two glaciers. However, comparison with mass balance measurements on e.g. Breiðamerkurjökull (Pálsson *et al.*, 2020) provides helpful constraints, as it covers the elevation range seen in the ablation areas of Kötlujökull and Sólheimajökull. The details of the cross sections, net balance values, balance velocities and travel times down both glaciers are given in Appendix A. The results for ice-flow velocity are presented in Figure 4 (b and c). Two velocity values are used: (1) The average velocity that assumes the same, constant velocity over each cross section, and (2) a maximum velocity. As ice flow will be slower near the glacier bed and its margins on both sides (e.g. Cuffey and Paterson, 2010), the average is an underestimate of the velocity transporting the tephra on and near the central flow-line of the glacier. To account for this we use a maximum velocity of 1.25 times the mean (Figure 4b and c). This value is based on the analysis of the actual transfer of the layer down the outlet glaciers and its comparison with the calculated balance velocities (Appendix A).

Changes to tephra layer thickness caused by ice-flow are to a first order expected to be mainly due to pure shear (vertical compression and horizontal elongation) above the equilibrium line. In contrast, simple shear (deformation due to gradients in velocity perpendicular to flow resulting in differential movement of parallel planes in the ice) is expected to be important near the edges and the bottom (Hudleston, 2015) but should be relatively minor elsewhere. We therefore expect that stretching and thinning of a tephra layer mainly occurs during its flow through the accumulation area. Thus, the total thinning during transport from the point of deposition of tephra to the point of maximum velocity will be the same as the ratio of the maximum velocity and the velocity at the location of fallout. The total amount of lateral transport in the direction of ice flow since the eruption can be estimated from the balance velocity of these two glaciers and this is summarized in Appendix A.

Kötlujökull: The 1918 tephra layer is presently exposed about 10 km below the equilibrium line (Figure 4a and 4b). The constraints described above put the most likely point of tephra fall 5–5.5 km above the equilibrium line, at an elevation of about 1300 m a.s.l. We put the most likely point slightly to the north of the present day flowline (Figure 4a), as ice flow for some years after the eruption would have been deflected southwards, towards the centre of the depression formed around the eruption site and described by the observers in 1919 (G. Sveinsson, 1919 and P. Sveinsson, 1930). The total lateral displacement is estimated to be about 15 km. A calculated maximum velocity of 470 m/yr occurs just below the equilibrium line while the velocity at the suspected place of fallout is approximately 65–70 m/yr, resulting in an estimate of total stretching and thinning of the tephra layer by a factor of 6.5, with the 35 cm thick layer exposed now translating to an original fallout thickness of$\sim$230 cm.

Sólheimajökull: Using the same approach as for Kötlujökull, with the layer exposed at 8–9 km below the equilibrium line, the estimated location of fallout lies 2–3 km above the equilibrium line and total transport down-glacier is estimated as about 11 km. The calculated maximum velocity of 250 m/yr occurs close to the equilibrium line while velocity at the location of fallout is about 70 m/yr, stretching by a factor of $\sim$3.6, and an initial layer thickness of $\sim$120 cm.

Sléttjökull: In contrast to the valley-confined outlets, the broad, lobe-like geometry and much lower balance velocities at Sléttjökull (15–25 m/year), result in displacements of 1.5–2 km since 1918 and insignificant thinning.

These results have considerable uncertainty, both in terms of fallout location and initial thickness. It is likely that disturbance to ice flow near the eruption site in 1918 was considerable, possibly resulting in lower flow velocities in Kötlujökull in the first years after the eruption, similar to what was observed within the depression formed in the Gjálp eruption in Vatnajökull in 1996 (Jarosch *et al.*, 2008). Despite this uncertainty, we consider the overall results robust, and that the tephra now exposed on the lower parts of the outlet glaciers of Kötlujökull and Sólheimajökull fell inside the caldera and has experienced a large amount of thinning.

Isopach map

The isopach map, based on all available data (Figures 1–4) and our reconstructed locations and thicknesses inside the caldera, is shown in Figures 5 and 6, with the latter being a blowup covering Mýrdalsjökull. Figure 6 shows the isopachs and the estimated locations of fallout and calculated thicknesses of tephra at these sites. The map in Figure 5 shows that no single direction was dominant in the distribution of tephra from this eruption. Three dispersal axes are most prominent, directed towards north, northeast and southeast. Three other axes are indicated by the map, towards south, west and northwest. The 1 cm isopach extends about 100 km to the north but less than 10 km to the southwest. Details of how dispersal of tephra varied with time during the eruption are given in Larsen *et al.* (this issue).

Volume of airborne tephra in 1918

The bulk volume of the tephra carried by the plume and forming the tephra layer has been estimated by: (1) direct integration of the map for contours >0.5 cm, using Surfer (Golden Software) after generating the map using the kriging option. (2) Plotting the logarithm of thickness against the square root of the area within each isopach and integrating the curve as four exponential segments, following Fierstein and Nathenson (1992) (Figure 7a). (3) By integrating between successive contours we obtain 10 exponential segments. In all cases, the fallout outside the outermost, 0.5 cm isopach, was estimated by extrapolating the exponential curve obtained for the interval between 1 and 0.5 cm out to infinity.

The results on volume by the three methods (Table 1) all lie in the range 0.9 to 1.0 km^3. They are not fully independent, as the same method is used in all cases for the region outside the 0.5 cm contour. Integration of the map also shows that about half of the total volume of airborne tephra (0.45 – 0.50 km^3) fell on Mýrdalsjökull.

The uncertainty of the volume estimate of tephra that fell on Mýrdalsjökull can be crudely estimated. The tephra thickness near the vents on Figure 2a has an estimated uncertainty of 40%, while thicknesses for the northern part (Sléttjökull) are better constrained due to the limited effect of post 1918 ice flow on layer thickness, as shown above. By using uncertainties of 40% for the caldera and 20% for the northern part of the glacier, the resulting combined error for the glacier part is 0.15 km^3. For the areas outside the glacier, the large number of survey points results in lower uncertainty, which we cautiously assume to be no more than 20%, or 0.1 km^3. By using the mean of the three values in Table 1 as the best available estimate for the tephra layer we obtain a rounded off volume of 0.95$\pm$0.25 km^3.

Table 1. Estimates of the bulk volume of the Katla 1918 tephra layer. – *Rúmmál gjóskulagsins frá 1918.*

Thickness (cm)	Map integration[1] km^3	Exponential method 4 segments[2] km^3	Exponential method 10 segments[2] km^3
<0.5	(0.16)	0.16	0.16
>0.5	0.74	0.84	0.87
Total	0.90	1.00	0.93

[1]Integration made using Surfer (Golden Software) for thickness >0.5 cm and exp. integration results for <0.5 cm.
[2]The fallout thickness as function of the square root of area is shown on Figure 7a.

Fallout in the ocean to the south and southeast of the volcano is estimated as about 10% of the total, a value obtained from integration of the ocean part of the map in Figure 5. We estimate the total mass of the layer using a density of 1200 kg/m^3, a reasonable number for basaltic, fine grained, and to a large degree phreatomagmatic tephra (Oddsson *et al.*, 2012). The result is a tephra layer deposit mass of 1.15$\pm$0.30$\times$10^{12} kg (about 0.4$\pm$0.1 km^3 DRE).

It should be noted that the volume/mass obtained here is far from being the total amount of material produced in the eruption, as water-transported pyroclasts are not included. This material may have been of comparable quantity (Tómasson, 1996; Larsen, 2000) as that of the airborne tephra. Moreover, any material deposited at the eruption site, forming a subglacial edifice, is not included.

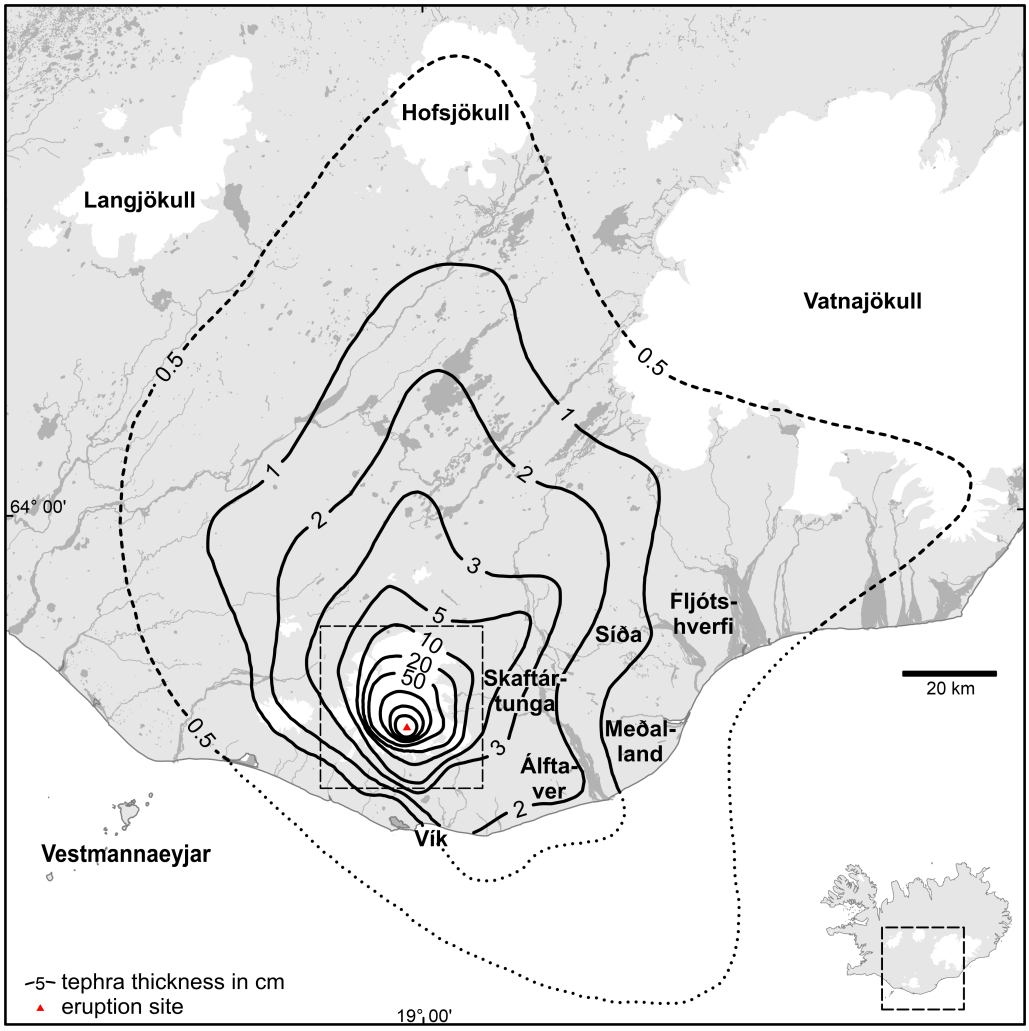

Figure 5. Isopach map of the Katla 1918 tephra layer based on available data and the reconstructed thicknesses and locations within the Katla caldera. The frame marks the area shown in Figure 6. – *Jafnþykktarkort af gjóskulaginu frá 1918, byggt á öllum tiltækum mælingum og reiknuðum þykktum og staðsetningum innan Kötluöskjunnar. Ramminn afmarkar kortið á 6. mynd.*

DISCUSSION

When compared with published estimates of previous eruptions (Óladóttir *et al.*, 2018), the results obtained demonstrate that Katla 1918 is among the largest of the tephra layers produced by Katla in the last 1000 years. A previous estimate was made in 1919 by Samúel Eggertsson (1919) using the approximation of a stack of concentric vertical cylinders with Katla at their axis and height equal to tephra thickness. Eggertsson's result was a total volume of 0.7 km^3. Given the scarce data available at this time this estimate must be regarded as remarkably good. In Figure 7b the layer is compared with other Katla layers that fell mostly on land and have been mapped (Óladóttir *et al.*, 2018). The data from the older eruptions does not include the thick proximal part, allowing compar-

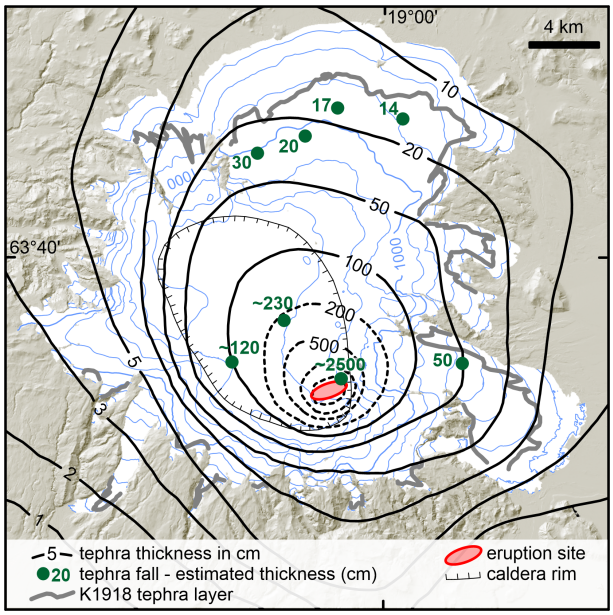

Figure 6. The isopach map for the Mýrdalsjökull ice cap with the eruption site and estimated location of fallout and thickness of the tephra presently exposed in Kötlujökull, Sólheimajökull, Sléttjökull and the observation by P. Sveinsson (1930) in September 1919 of 50 cm thickness on Kötlujökull. The point by the eruption site is the approximate location of the tephra piles shown in Figure 2. – *Jafnþykktarkort af gjóskulaginu frá 1918 á Mýrdalsjökli. Kortið sýnir einnig staði þar sem gjóskan sem sem fannst í Kötlujökli og Sólheimajökli er talin hafa fallið, ásamt reiknaðri upphaflegri þykkt á sömu stöðum. Þykktin (50 cm) á miðjum Kötlujökli er samkvæmt mælingu Páls Sveinssonar í september 1919.*

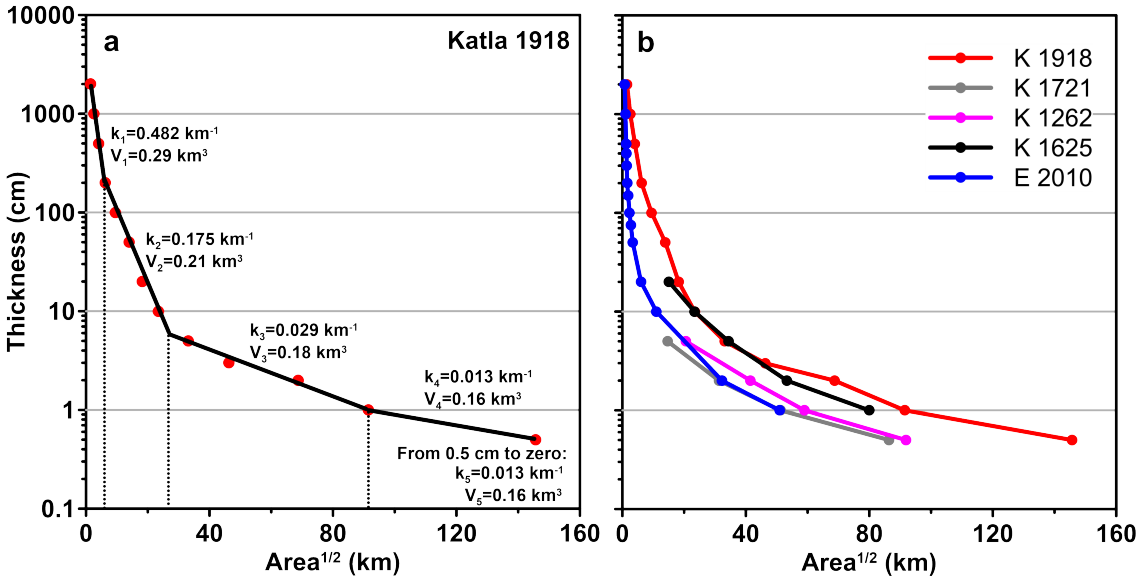

Figure 7. a) Plot of tephra thickness for the Katla 1918 layer as a function of the square root of the area. Here the layer is imaged using four segments and integration of the segments (Fierstein and Nathenson, 1992) yields a total volume estimate of 1.0 km^3. b) Comparison of Katla 1918 with the Katla tephra layers of 1262, 1625 and 1721, based on isopach maps in Larsen (2000) and Óladóttir *et al.* (2018). – *a) Þykkt gjóskulagsins frá 1918 sem fall af kvaðratrót af flatarmáli svæðis innan hverrar jafnþykktarlínu. Hér er þykktardreifing nálguð með fjórum beinum línum og rúmmálið reiknast 1.0 km^3. b) Samanburður K1918 við Kötlulögin frá 1262, 1625 og 1721.*

ison only for isopachs in the range 1–20 cm, but they indicate that Katla 1918 may be slightly larger than Katla 1625, and considerably larger than the layers from 1262 and 1721. For comparison, the tephra layer from Eyjafjallajökull in 2010 (bulk volume 0.27 km^3) is also shown (Gudmundsson, *et al.*, 2012). This indicates that the Katla 1918 layer was about four times more voluminous than Eyjafjallajökull in 2010 and it had almost five times the bulk volume of the Hekla 1947 tephra layer (0.21 km^3, Thorarinsson, 1968). This confirms that Katla 1918 is the largest explosive eruption in Iceland since the rhyolitic Askja 1875 eruption (Carey *et al.*, 2009).

The results indicate that about half of the airborne tephra was deposited on Mýrdalsjökull. It is likely that for the weaker eruptions of Katla, e.g. the eruptions in the 19th century (Thorarinsson, 1975), a relatively minor proportion of the tephra erupted was deposited outside the ice cap.

The large thickness of tephra on Mýrdalsjökull is not surprising, given the large proximal thicknesses observed in recent eruptions in Grímsvötn and Eyjafjallajökull. In the eruption in Grímsvötn in 2004 (Jude-Eton *et al.*, 2012; Oddsson *et al.*, 2012) where the bulk volume of tephra was only 0.02 km^3, proximal thickness was 7–8 m, and in the eruption in Eyjafjallajökull in 2010 (Gudmundsson *et al.*, 2012, bulk tephra volume 0.27 km^3), the maximum proximal thickness was about 30 m. The Katla 1918 eruption lasted 23 days with varying activity at the vents, and pervasive magma-water interaction. The dispersive power of the weaker phases of the eruption is expected to have been low, with most of the tephra deposited not far from the vents, contributing to thick proximal, predominantly phreatomagmatic deposits. It is likely that this also holds for several of the previous Katla eruptions considered by Óladóttir *et al.* (2018) and Schmith *et al.* (2018).

The assessments made here of stretching and thinning of tephra layers exposed in the lower half of the ablation areas of glaciers may prove useful for estimating the original thickness of older, ice-covered tephra layers. This may for instance apply in Vatnajökull, where several tens of tephra layers from the last eight centuries are exposed in the outlet glaciers (Larsen *et al.*, 1998) and ice core drilling has confirmed how tephra layers are preserved in the accumulation areas (Steinþórsson, 1977).

CONCLUSIONS

A first comprehensive isopach map of the tephra layer formed in the eruption of Katla in 1918 is presented, based on sampling spanning almost eight decades. The key findings are:

1. The volume of airborne tephra erupted is estimated as 0.95±0.25 km^3, indicating that Katla 1918 is the most voluminous explosive eruption in Iceland since the rhyolitic eruption of Askja in 1875.
2. Tephra near the vents in the easternmost part of the Katla caldera was 20–30 m thick, and the tephra exceeded 1 m thickness over large parts of the 100 km^2, ice-filled caldera.
3. About 50% of the tephra fell within Mýrdalsjökull ice cap. Most of the tephra fell on land; only about 10% fell into the ocean.
4. The tephra fall is mostly fine-grained, consistent with phreatomagmatic fragmentation being dominant for long periods during the eruption. A substantial part of the erupted material was water -transported. This material is not considered here. Hence, the results do not provide and estimate of the total magma erupted.

Acknowledgements

MHJ acknowledges an EU Marie Skłodowska-Curie fellowship in 2016–2018. The work of JG was supported by an Icelandic Research Fund, Landsvirkjun and Fræðslusjóður Suðurlands, and that of TJ by the GOSVÁ program on volcanic hazard assessment in Iceland. The field effort in 2018 was supported by the Chief of Police in South Iceland, (Lögreglustjórinn á Suðurlandi) and the Icelandic Road Authority (Vegagerðin). Joaquin Beloz at the Icelandic Geodetic Survey gave us access to the oblique air photos from 1937. MTG and ÞH acknowledge support from the University of Iceland Research Fund. Finally we also would like to thank Olgeir Sigmarsson and our many colleagues and friends that have throughout the years given a hand in the fieldwork. Constructive reviews

by Judy Fierstein and two anonymous reviewers significantly improved the quality of this publication.

ÁGRIP

Kötlugosið 1918 ásamt hlaupinu mikla sem gosið olli og flæddi yfir Mýrdalssand, Álftaver og Meðalland, var einn af stærstu atburðum í náttúru Íslands á 20. öld. Lengi hefur verið vitað að gjóskugosið var mikið enda barst gjóska vítt og breitt um landið meðan á því stóð. Gosið varð síðla hausts eftir að gróður var kominn í vetrardvala auk þess sem gjóskan féll víða á bert land þar sem varðveisluskilyrði voru ekki góð. Því hefur heildstætt þykktarkort af gjóskulaginu vantað. Mælingar hafa verið gerðar í áratugi á gjóskulaginu frá 1918 á svæðum umhverfis Mýrdalsjökul og miklum gögnum safnað, en upplýsingar hefur vantað frá jöklinum. Í tilefni af 100 ára afmæli gossins, var ráðist í það í ágúst 2018 að safna skipulega sýnum og mæla þykktir á norðanverðum Mýrdalsjökli þar sem gjóskulagið kemur úr jökli, 2–3 km ofan jökuljaðars, og á völdum svæðum í nágrenni jökulsins. Sumarið 2012 hafði sýnum verið safnað af Sólheimajökli og Kötlujökli, þykktir mældar og sýni tekin. Að auki hafa lýsingar og myndir úr ferðum á Mýrdalsjökul að gosstöðvunum sumarið og haustið 1919, árið eftir gosið, nýst til að staðsetja gosstöðvar og meta gjóskuþykktir á jöklinum nærri þeim. Upplýsingar sem til eru um ísþykkt og mælingar á ísskriði frá 2001 eru síðan notaðar ásamt þekkingu á afkomu jökulsins til að reikna ferðatíma íss af ákomusvæðum Kötlujökuls og Sólheimajökuls niður undir sporða, þar sem gjóskan frá 1918 kemur upp úr jöklinum. Þessir reikningar benda til þess að gjóskan sem nú er neðarlega í Kötlujökli hafi fallið inni í Kötluöskjunni, 5 km ofan jafnvægislínu í um 1300 m hæð, 5 km norðvestan við gosstöðvarnar. Gjóskan neðst í Sólheimajökli er talin hafa flust til um $\sim$11 km og hafa fallið um 6 km vestan gosstöðvanna. Með mati á jafnvægishraða ísflæðis á þessum tveimur jöklum fæst að gjóskan sem nú er í Kötlujökli hafi verið rúmlega 2 m þykk í lok gossins, eða 6–7 sinnum þykkari en hún er nú niðri á leysingasvæðinu. Breytingin í þykkt stafar af því að við hraðaaukningu íssins þynnist lagið jafnframt því að það teygist á því. Fyrir Sólheimajökul gæti lagið hafa verið 3–4 sinnum þykkara þar sem það féll og e.t.v. um 1.2 m á þykkt. Ljósmyndirnar frá haustinu 1919 benda til þess að gjóskubunkinn upp við gosstöðvarnar hafi verið um 25 m þykkur. Þessar upplýsingar eru tengdar við þær fjölmörgu mælingar sem gerðar hafa verið utan jökulsins og fæst þannig heildstætt þykktarkort af gjóskulaginu. Samkvæmt reikningum á stærð lagsins er rúmmál þess 0.95 ± 0.25 km^3, og því stærra en önnur gjóskulög sem fallið hafa á Íslandi eftir Öskjugosið 1875. Þessar tölur segja þó ekki alla söguna um stærð gossins, því gosefni sem bárust með hlaupinu eru ekki talin með og ekki er reynt að leggja mat á tilvist eða stærð mögulegs eldvarps á gosstöðvunum undir jöklinum. Vatnsbornu gosefnin gætu verið sambærileg að magni og loftborna gjóskan sem metin er hér, meðan eldvarp sem kann að hafa myndast er sennilega miklu minna en magn loftborinnar og vatnsborinnar gjósku.

REFERENCES

Ágústsson, H., H. Hannesdóttir, Th. Thorsteinsson, F. Pálsson and B. Oddsson 2013. Mass balance of Mýrdalsjökull ice cap accumulation area and comparison of observed winter balance with simulated precipitation. *Jökull* 63, 91–104.

Belart, J. M. C., E. Magnússon, E. Berthier, Á. Þ. Gunnlaugsson, F. Pálsson, G. Aðalgeirsdóttir, T. Jóhannesson, Th. Thorsteinsson, H. Björnsson 2020. Mass balance of 14 icelandic glaciers, 1945–2017: Spatial variations and links with climate. *Front. Earth Sci.*, 8, 163.

Bjarnason, H. and S. Thorarinsson 1940. Datering av vulkaniska asklager I isländsk jordmån. *Geografisk Tidskrift* 43, 5–30.

Björnsson, H. 1979. Glaciers in Iceland. *Jökull* 29, 74–80.

Björnsson, H., F. Pálsson and M. T. Gudmundsson 2000. Surface and bedrock topography of Mýrdalsjökull ice cap, Iceland: The Katla caldera, eruption sites and routes of Jökulhlaups. *Jökull* 49, 29–46.

Carey, R., B.F. Houghton, Th. Thordarson 2009. Tephra dispersal and eruption dynamics of wet and dry phases of the 1875 eruption of Askja volcano, Iceland. *Bull. Volc.* 72, 259–278.

Cuffey, K. and W. S. B. Paterson 2010. *The physics of glaciers.* 4th edition. Academic Press, 693 pp.

Duller, R.A., N. P. Mountney, A. J. Russell and N. C. Cassidy 2008. Architectural analysis of a volcaniclastic jokulhlaup deposit, southern Iceland: sedimentary evidence for supercritical flow. *Sedimentology* 55, 939–964.

Eggertsson, S. 1919. Ýmislegt smávegis viðvíkjandi Kötlugosinu 1918 (Some points about the Katla 1918 eruption). *Eimreiðin* 1919, 212–222.

Einarsson, P. and B. Brandsdóttir 2000. Earthquakes in the Mýrdalsjökull area, Iceland, 1978–1985: Seasonal correlation and connection with volcanoes. *Jökull* 49, 59–74.

Eyþórsson, J. 1945 Um Kötlugjá og Mýrdalsjökul. (In Icelandic: On Kötlugjá canyon and Mýrdalsjökull). *Náttúrufræðingurinn* 15, 145–174.

Fierstein J. and M. Nathenson 1992. Another look at the calculation of fallout tephra volumes. *Bull. Volc.* 54, 156–167.

Gudmundsson, M. T. and Th. Högnadóttir 2001. *Gögn um Kötlugosið 1918: Ljósmyndir Kjartans Guðmundssonar úr ferðum á Mýrdalsjökul í júní og september 1919.* (Data on the Katla eruption of 1918: The photos by Kjartan Guðmundsson from trips to Mýrdalsjökull in June and September 1919). Raunvísindastofnun Háskólans, report RH-08-2001, 19 pp.

Gudmundsson, M. T., F. Sigmundsson, H. Björnsson and Th. Högnadóttir 2004. The 1996 eruption at Gjálp, Vatnajökull ice cap, Iceland: efficiency of heat transfer, ice deformation and subglacial water pressure. *Bull. Volcanology* 66, 46–65.

Gudmundsson, M. T., J. Elíasson, G. Larsen, Á. G. Gylfason, P. Einarsson, T. Jóhannesson, K. M. Hákonardóttir and H. Torfason 2005. Yfirlit um hættu vegna eldgosa og hlaupa frá vesturhluta Mýrdalsjökuls og Eyjafjallajökli. (in Icelandic: Overview of hazard due to eruptions and jökulhlaups from western Mýrdalsjökull and Eyjafjallajökull.) In: Gudmundsson, M. T. and Á. G. Gylfason (eds.): *Hættumat vegna eldgosa og hlaupa frá vestanverðum Mýrdalsjökli og Eyjafjallajökli.* Ríkislögreglustjórinn og Háskólaútgáfan, 11–44.

Gudmundsson, M. T., G. Larsen, Á. Höskuldsson and Á. G. Gylfason 2008. Volcanic hazard in Iceland. *Jökull* 58, 251–268.

Gudmundsson, M. T., T. Thordarson, Á. Höskuldsson, G. Larsen, H. Björnsson, A. J. Prata, B. Oddsson, E. Magnússon, T. Högnadóttir, G. N. Pedersen, C. L. Hayward, J. A. Stevenson and I. Jónsdóttir 2012. Ash generation and distribution from the April-May 2010 eruption of Eyjafjallajökull, Iceland. *Scientific Rep.* 2, 572. www.doi.org/10.1038/srep00572

Gudmundsson, Ó., B. Brandsdóttir, W. Menke and G. E. Sigvaldason 1994. The magma chamber of the Katla volcano in south Iceland revealed by 2-D seismic undershooting. *Geophys. J. Int.* 119, 277–296.

Hudleston, P. J. 2015. Structures and fabrics in glacial ice: a review. *J. Struct. Geol.* 81, 1–27.

Jaenicke, J., C. Mayer, K. Scharrer and U. Münzer 2006. The use of remote-sensing data for mass-balance studies at Mýrdalsjökull ice cap, Iceland. *J. Glaciol.* 52, 565–573.

Jarosch, A. H., M. T. Gudmundsson, T. Högnadóttir and G. Axelsson 2008. The progressive cooling of the hyaloclastite ridge at Gjálp, Iceland, 1996–2005. *J. Volc. Geoth. Res.* 170, 218–229.

Jóhannsson, G. 1919. *Kötlugosid 1918.* Bókaverslun Ársæls Árnasonar, Reykjavík, 72 pp.

Jóhannesson, T., H. Björnsson, E. Magnússon, S. Guðmundsson, F. Pálsson, O. Sigurðsson, Th. Thorsteinsson and E. Berthier 2013. Ice-volume changes, bias estimation of mass-balance measurements and changes in subglacial lakes derived by lidar mapping of the surface of Icelandic glaciers. *Ann. Glaciology* 54, 63–74.

Jónsdóttir, T. 2015. *Grain size distribution and characteristics of the tephra from the AD 871±2 Vatnaöldur and Katla 1918 eruptions, Iceland.* MS-thesis, Univ. of Iceland, Reykjavík, 142 pp.

Jónsson, G. and L. Kristjánsson. 2000. Aeromagnetic measurements over Mýrdalsjökull and vicinity. *Jökull* 49, 47–58.

Jónsson, G. 2008. Ferð að Kötlugjá haustið 1919. (In Icelandic: An inspection of Kötlugjá in the autumn of 1919). *Dynskógar* 11, 187–190.

Jude-Eton, T. C., Th. Thordarson, M. T. Gudmundsson and B. Oddsson 2012. Dynamics, stratigraphy and proximal dispersal of supraglacial tephra during the ice-confined 2004 eruption at Grímsvötn volcano, Iceland. *Bull. Volc.* 74, 1057–1082. www.doi.org/10.1007/-s00445-012-0583-3

Larsen, G. 2000. Holocene eruptions within the Katla volcanic system, south Iceland: Characteristics and environmental impact. *Jökull* 49, 1–28.

Larsen, G. 2018. *Jökulhlaup til austurs og suðurs frá Mýrdalsjökli I. Kötluhlaup eftir 1600: Umfang, hlaupleiðir, tjón og umhverfisbreytingar.* Research Report RH-13-2018, Science Institute, University of Iceland, 66 pp.

Larsen, G., M. T. Gudmundsson and H. Björnsson 1998. Eight centuries of periodic volcanism at the center of the Iceland hot spot revealed by glacier tephrastratigraphy. *Geology* 26, 943–946.

Larsen, G., A. J. Newton, A. J. Dugmore and E. G. Vilmundardóttir 2001. Geochemistry, dispersal, volumes

and chronology of Holocene from the Katla volcanic silicic tephra layers system, Iceland. *J. Quaternary Sci.* 16, 119–132.

Larsen, G., M. H. Janebo and M. T. Gudmundsson 2021. The explosive basaltic Katla eruption in 1918, south Iceland I: course of events, tephra fall and flood routes. *Jökull* 71, 1–20.

Mackintosh, A. N., A. J. Dugmore, F. M. Jacobsen 2000. Ice-thickness measurements on Sólheimajökull, south Iceland and their relevance for its recent behaviour. *Jökull* 48, 9–15.

Magnússon, E., M. T. Gudmundsson, G. Sigurdsson, M. J. Roberts, F. Höskuldsson and B. Oddsson 2012. Ice-volcano interactions during the 2010 Eyjafjallajökull eruption, as revealed by airborne radar. *J. Geophys. Res.* 117, B07405. https://doi.org/10.1029/2012JB009250

Mayer, C., J. Jaenicke, A. Lambrecht, L. Braun, C. Völksen, C. Minet and U. Münzer 2016. Local surface mass-balance reconstruction from a tephra layer - a case study on the northern slope of Mýrdalsjökull, Iceland. *J. Glaciol.* 63, 79–87. https://doi.org/10.1017/-jog.2016.119

Oddsson, B., M. T. Gudmundsson, G. Larsen and S. Karlsdóttir 2012. Monitoring the plume from the basaltic phreatomagmatic 2004 Grímsvötn eruption – application of weather radar and comparison with plume models. *Bull. Volc.* 74, 1395–1407.

Oddsson, B., M. T. Gudmundsson, B. R. Edwards, T. Thordarson, E. Magnússon and G. Sigurdsson 2016. Subglacial lava propagation, ice melting and heat transfer during emplacement of an intermediate lava flow in the 2010 Eyjafjallajökull eruption. *Bull. Volc.* 78, 48. https://doi.org/10.1007/s00445-016-1041-4

Óladóttir, B. A., O. Sigmarsson, G., Larsen and T. Thordarson 2008. Katla volcano, Iceland: Magma composition, dynamics and eruption frequency as recorded by tephra layers. *Bull. Volcanology* 70, 475–493. https://doi.org/10.1007/s00445-007-0150-5

Óladóttir, B. A., G. Larsen and O. Sigmarsson 2014. Volume estimates of nine prehistoric (∼1860 BC – 870 AD) Katla tephra layers. *Jökull* 64, 23–40.

Óladóttir, B. A., O. Sigmarsson and G. Larsen 2018. Tephra productivity and eruption flux of the subglacial Katla volcano, Iceland. *Bull. Volc.* 80, 58.

Pálsson, F., A. Gunnarsson, G. Jónsson, H. S. Pálsson and S. Steinþórsson 2020. *Vatnajökull: Mass balance, meltwater drainage and surface velocity of the glacial year 2018–19*. Report RH-01-20, 48 pp.

Pálsson, F., H. Björnsson and E. Magnússon 2005. *Rennslisleiðir vatns undir Kötlujökli (Höfðabrekkujökli).* (Water drainage paths beneath Kötlujökull). Report RH-04-05, 17 pp.

Schmith, J., A. Höskuldsson, P. M. Holm and G. Larsen 2018. Large explosive basaltic eruptions at Katla volcano, Iceland: Fragmentation, grain size and eruption dynamics. *J. Volcanol. Geoth. Res.* 354, 140–152.

Steinþórsson, S. 1977. Tephra layers in a drill core from the Vatnajökull ice cap. *Jökull* 27, 2–27.

Sturkell, E., P. Einarsson, M. J. Roberts, H. Geirsson, M. T. Gudmundsson, F. Sigmundsson, V. Pinel, G. B. Gudmundsson, H. Ólafsson and R. Stefánsson 2007. Seismic and geodetic insights into magma accumulation at Katla subglacial volcano, Iceland: 1999 to 2005. *J. Geophys. Res.* 113, B03212.

Sveinsson, G. 1919. *Kötlugosid 1918 og afleiðingar þess* (The Katla eruption of 1918 and its consequences). Prentsmidjan Gutenberg, Reykjavík, 61 pp.

Sveinsson, P. 1930. Kötluför, 2. september 1919. (In Icelandic: A trip to Katla on 2nd of September 1919). In: Björnsson, B. (ed.). *Vestur-Skaftafellssýsla og íbúar hennar*, 67–73.

Thorarinsson, S. 1944. Tefrokronologiska Studier på Island. *Geografiska Annaler* 26, 1–217.

Thorarinsson, S. 1958. The Öræfajökull eruption of 1362. *Acta Nat. Isl.* II–2, 1–100.

Thorarinsson, S. 1968. *Heklueldar* (in Icelandic: Hekla fires). Sögufélagið. Reykjavík, 185 pp.

Thorarinsson, S. 1975. Katla og annáll Kötlugosa (in Icelandic: Katla and an annal of Katla eruptions). *Árbók Ferðafélags Íslands* 1975, 125–149.

Thorarinsson, S. 1981. *The application of tephrochronology in Iceland.* In: Self, S. and R. S. J. Sparks (eds.). Tephra Studies. D. Reidel Publishing Company, Dordrecht, 109–134.

Tómasson H. 1996. The Jökulhlaup from Katla in 1918. *Ann. Glaciology* 22, 249–254.

Þorkelsson, K., Á. G. Gylfason, J. Elíasson and M. T. Gudmundsson 2005. Hættumat vegna eldgosa og hlaupa frá vestanverðum Mýrdalsjökli og Eyjafjallajökli, samantekt og tillögur stýrihóps (In Icelandic: Hazard assessment due to eruptions and jökulhlaups from western Mýrdalsjökull and Eyjafjallajökull, summary and recommendation of steering group). In: Gudmundsson, M. T. and Á. G. Gylfason (eds.): *Hættumat vegna eldgosa og hlaupa frá vestanverðum Mýrdalsjökli og Eyjafjallajökli*, Ríkislögreglustjórinn og Háskólaútgáfan, 9–10.

Appendix A: Estimates of balance velocities for Kötlujökull and Sólheimajökull

The balance velocities for the outlet glaciers were estimated by using numbers from Ágústsson *et al.* (2013) on net balance on the accumulation areas, with the maximum set for Kötlujökull of 4.2 m water equivalent, and 3.2 m w.e. for Sólheimajökull. Area for each 100 m height interval was measured from the lidar-derived surface map of Mýrdalsjökull (Jóhannesson *et al.*, 2013), and the equilibrium lines set at 1000 m

Table A1: Kötlujökull – mass balance as a function of height, cross-sections, calculated balance velocities and travel times. – *Kötlujökull: Afkoma sem fall af hæð, þversnið og reiknaður jafnvægishraði og ferðatími.*

Elevation (m a.s.l.)	Area (km^2)	Net balance w.e. (m)	Net balance ice (m)	B (ice) (10^6 m^3)	Sum of B (ice) (10^6 m^3)	Section width (m)	Mean ice thickn. (m)	Cross-section (m^2)	Mean velocity (m/yr)	Max velocity (m/yr)	Distance from ice divide (km)	Travel time (years)
1500-1400	4.2	4.2	4.62	19.4	19.4				0	0	0.0	
1400-1300	32.5	3.8	4.18	135.7	155.1	5600	480	2688000	58	72	3.0	
1300-1200	18.5	3.4	3.74	69.1	224.2	3000	475	1425000	158	197	6.0	29
1200-1100	7.4	2.5	2.75	20.3	244.5	2000	425	850000	288	360	7.4	6
1100-1000	3.8	0.8	0.88	3.3	247.9	2000	370	740000	336	420	8.2	2
1000-900	4.8	-0.8	-0.88	-4.2	243.7	2000	325	650000	376	469	9.5	3
900-800	5.5	-1.5	-1.65	-9.1	234.6	2000	350	700000	336	420	10.7	2
800-700	7.5	-2.4	-2.64	-19.8	214.8	2000	400	800000	269	336	12.7	5
700-600	5.1	-2.9	-3.19	-16.3	198.6	2000	385	770000	258	323	14.2	5
600-500	8.0	-3.9	-4.29	-34.3	164.3	4000	300	1200000	137	171	16.5	7
500-400	18.3	-4.9	-5.38	-98.5	65.7	10000	215	2150000	31	38	19.0	29
400-300	10.4	-6.0	-6.59	-68.6	-2.8	10000	150	1500000	0	0	20.3	
300-200	5.0	-7.2	-7.91	-39.6	-42.4							
Total area:	**131.0 km^2**		**Net balance:**			**-0.3 m/yr**	**Calculated travel time from 1300 m elevation:**					**88**

Table A2: Sólheimajökull – mass balance as a function of height, cross-sections, calculated balance velocities and travel times. – *Sólheimajökull: Afkoma sem fall af hæð, þversnið og reiknaður jafnvægishraði og ferðatími.*

Elevation (m a.s.l.)	Area (km^2)	Net balance w.e. (m)	Net balance ice (m)	B (ice) (10^6 m^3)	Sum of B (ice) (10^6 m^3)	Section width (m)	Mean ice thickn. (m)	Cross-section (m^2)	Mean velocity (m/yr)	Max velocity (m/yr)	Distance from ice divide (km)	Travel time (years)
1500-1400	4.6	3.2	3.52	16.2	16.2				0	0	0.0	
1400-1300	15.2	2.5	2.75	41.8	57.9	3500	300	1050000	55	69	2.3	
1300-1200	6.0	1.5	1.65	9.9	67.8	2000	250	500000	136	170	3.7	13
1200-1100	4.0	0.5	0.55	2.2	70.0	1600	220	352000	199	249	4.7	5
1100-1000	3.2	-0.5	-0.55	-1.8	68.3	2000	290	580000	118	147	5.7	5
1000-900	2.1	-2	-2.20	-4.6	63.6	1200	300	360000	177	221	6.5	4
900-800	1.9	-3	-3.30	-6.3	57.4	1300	250	325000	177	221	7.3	4
800-700	1.6	-4	-4.40	-7.0	50.4	1100	240	264000	191	238	8.1	3
700-600	1.6	-5	-5.49	-8.8	41.6	1000	300	300000	139	173	9.5	7
600-500	1.9	-6	-6.59	-12.5	29.0	1000	250	250000	116	145	11.3	11
500-400	1.6	-7	-7.69	-12.3	16.7	1000	250	250000	67	84	12.7	13
400-300	1.5	-8	-879	-13.2	3.5	1000	200	200000	18	22	13.9	26
300-200	0.9	-9	9.89	-8.9	-5.4	1000	180	180000	0	0	14.8	
200-100	0.3	-10	-10.99	-3.3	-8.7	1000	70	70000			15.5	
Total area:	**131.0 km^2**		**Net balance:**			**-0.2 m/yr**	**Calculated travel time from 1300 m elevation:**					**91**

Explanations: The ice drainage areas are shown on Figure 4a. and the cross sections are taken at elevation intervals of 100 m. Net balance of ice is obtained by dividing the water equivalent net balance with the ratio of densities of ice and water. B is obtained by multiplying the net balance (in m/yr) by the area. Distances are measured using the central flowlines (see Figure 4). – *Skýringar: Ísasvæðin eru á mynd 4a og þversnið eru tekin á hverju 100 m hæðarbili. Afkoma er fengin með því að deila í vatnsgildið með eðlismassahlutfalli íss og vatns. B fæst með því margfalda afkomuna með flatarmáli hvers hæðarbils. Fjarlægðir eru mældar eftir straumlínu í miðju hvors jökuls.*

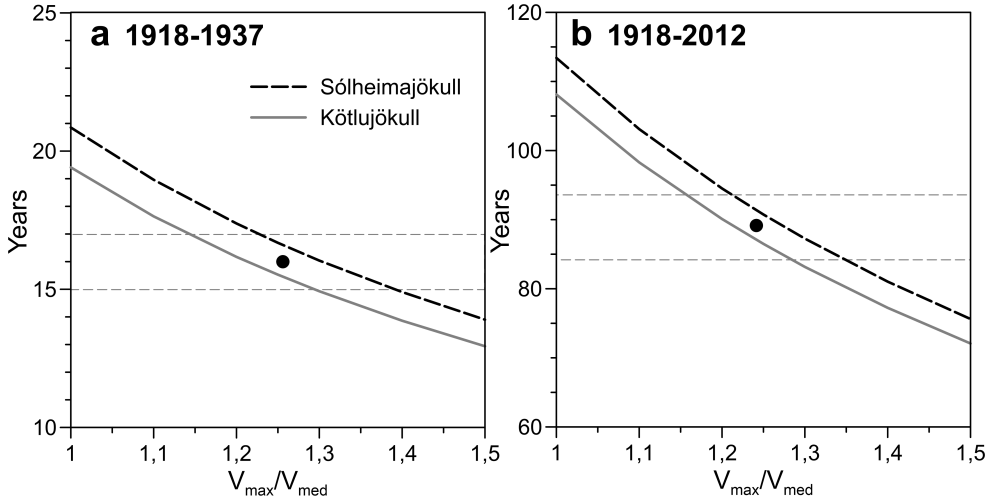

Figure A1. Sólheimajökull and Kötlujökull. Estimate of the ratio of the actual travel velocity of the layer (V_{max}) and the calculated balance velocity (V_{med}). – *Mat á hlutfalli reiknaðs jafnvægishraða og raunverulegs hraða gjóskulagsins niður Sólheimajökul og Kötlujökul.*

a.s.l. for Kötlujökull and 1100 m a.s.l. for Sóheimajökull. Cross sections through which ice flows were estimated from the surface map and bedrock maps (Björnsson *et al.*, 2000; Mackintosh *et al.*, 2000; Pálsson *et al.*, 2005). When estimating the width of the section for each glacier, the shallowest part along the sides was omitted in both outlet glaciers, as well as very thin ice over major obstacles. The balance values were adjusted, keeping the equilibrium line fixed, until a net balance of -0.2 to -0.3 m/yr was obtained. The calculations are presented in Tables A1 and A2. The numbers obtained indicate that the net mass balance in the accumulation area of Sólheimajökull is somewhat lower than for Kötlujökull, in broad agreement with the findings of Ágústsson *et al.* (2013). Moreover, higher ablation is required for the lower parts of Sólheimajökull than for Kötlujökull to obtain the slightly negative mass balance. It is beyond the scope of this work to elaborate on possible explanations, but less extensive tephra cover on the lower parts of Sólheimajökull, coupled with it facing south while Kötlujökull faces east, are among possible explanations for this difference.

The fact that the tephra layer emerges from the ice through surface ablation proves that it must have fallen on the accumulation areas, above the equilibrium line. An estimate of the location of fallout for the tephra exposed at each glacier can therefore be obtained by finding the approximate travel time below the equilibrium line from the velocity values, subtracting the result from the time since the eruption (94 years for sampling in 2012), and then use the velocities above the equilibrium line to estimate the distance of travel in the accumulation areas. Time of transfer, t_i, along a central flowline between points defined by a 100 m surface height difference is estimated assuming a linear change in flow velocity with distance. If the velocity at the up-slope boundary is v_i and at the downslope boundary v_{i+1} of the longitudinal section of length x, the distance travelled over time dt is dx, or

$$dx = (v_i + \text{ax}\ )\ dt \qquad (1)$$

As the change in velocity is assumed linear the gradient in velocity over distance is defined as $a = (v_{i+1} - v_i)/x$, where v_i and v_{i+1} are respectively

the ice velocities at the up-slope and down-slope ends of the longitudinal section. Inserting a into (1), solving for dt and integrating, the result is

$$t_i = \frac{x}{v_{i+1} - v_i} ln\left[\frac{v_{i+1}}{v_i}\right] \quad (2)$$

Tables A1 and A2 show travel times for each 100 m height interval between 1300 m and 400 m elevation on Kötlujökull and 1300 m to 300 m on Sólheimajökull. The results indicate travel times of 88 years for Kötlujökull and 91 year for Sólheimajökull, slightly less than the 94 years between eruption and time of sampling assuming that the velocity was 1.25 times the calculated average balance velocity. This value of 1.25 is derived by finding the velocity that best fits the location of the tephra layer in the two outlet glaciers in 1937 and 2012.

The 1937 position is estimated from aerial photos taken by the Danish Geodetic Institute. Figure A1a shows the best fitting estimate for the velocity over the period 1918–1937. Figure A1a shows the calculated travel time from the equilibrium line (6.4 km for Kötlujökull, 3.8 km for Sólheimajökull). Since the layer emerged from within the ice in 1937 as indicated schematically in Figure 4b, it is assumed that it must have originated within the accumulation area and experienced burial for a minimum of 2–4 years. The travel time within the ice of the ablation area is therefore estimated to have been 15–17 years (horizontal dashed lines in Figure A1a). This is achieved with V_{max}/V_{med} = 1.26.

For the period 1918–2012, figure A1b shows the calculated total travel time from the 1300 m contour down to the location of the tephra layer in 2012. Assuming that the time of transport above the location of the 1300 m contour was between zero and 10 years, travel time from the 1300 m contour was 84–94 years (horizontal dashed lines in Figure A1b). The best fitting estimate is V_{max}/V_{med} = 1.24. The value of 1.25 is the mean of the values for 1937 and 2012. For Kötlujökull the calculated time of travel through the ablation area of the tephra that become exposed in 2012, is about 50 years and just over 70 years at Sólheimajökull. Although these values have considerable uncertainty they constrain the fallout locations to specific regions in the accumulation areas.